Modelling, Simulation and Conception of Parallel Climbing Robots for Construction and Service

R. Saltarén, R. Aracil, J. M. Sabater, O. Reinoso, L. M. Jimenez,
Miguel Hernández University,
Dep. of Industrial Systems Engineering , Campus of Elche, 03202. Elche (Alicante), Spain
roque.saltaren@umh.es

Abstract. In this paper we present a research work on the use of parallel platforms as climbing robots considering the big load capacity that this type of structures have and their ability to progress on the workspace. In the first part we suggest a theoretic framework for the numerical calculation of the inverse and direct kinematics based on a multybody dynamics model. The dynamics of a parallel platform is modelling and simulate using a simulation package. With base in these simulations, we calculate the capacity necessary in the actuators to achieve a set of configurations that typically will be presented in a displacement along a structural frame.

Keywords: Robotics, climbing robots, construction robots, parallel robots, field robotics.

1. INTRODUCTION

Typically, walking and climbing robots base their displacement on the movement of their legs (1), (2). In most of the mentioned robots, legs are made of serial-connected articulated links. It is remarkable that the use of legs on climbing robots implies a great number of degrees of freedom, with motors and sensors for each one of them, increasing the complexity of control, the machine weight and cost.

On climbing robots, availability of a great number of redundant degrees of freedom does not necessarily increase the ability of the machine to progress on the workspace. An important number of the degrees of freedom of a climbing robot stay hold to be used as a base to the body and as reference for the legs that at this moment are operating as an advance mechanism. Architecture of serial legs also implies a limit on load charge, what is a typical effect on serial articulated mechanisms influenced by force and torque effects that are present on joints and so that on the capacity of power actuators, (7). Due to the preceding, it is also noticeable that relations weight/power on climbing robots are high and the useful load capacity and the velocity of these mechanism are limited.

To summarize, technical characteristics of climbing robots with legs implies limits that are capable of improvement:

- Use of a great number of DOF, with few of them on movement and working in a combined way.
- Limited use of the DOF and of the available total power.
- High weight, that limits the relation weight/power and the velocity of robot.
- Limited capacity for using with high weight loads.
- Not use of power actuators as structural elements.

To solve some of the preceding problems, this paper suggest some mechanical structures based on parallel platforms with 6 degrees of freedom. Parallel platforms present the following advantages that made them especially suitable to work as climbing robots:

- Power actuators are connected directly to the base of robot, what is the final effector. Therefore, the power actuators are used as structural elements and they work simultaneously, that implies the capacity of manipulating higher loads than their own weight.
- Parallel structures are mechanisms that offer a high stiffness, with low weight and high operating velocity, compared with any other kind of robotic structure.
- To define one's position, and to point itself inside the workspace, parallel structures need 6 DOF. Using all the degrees of freedom for the displacement, the proposed climbing robots use a minimum number of power actuators, comparing with other types of climbing robots.

2. THEORETIC FRAME FOR RRPS PARALLEL PLATFORMS

The type of robots proposed in this paper are based on a parallel platform with 6 degrees of freedom (7), with a **RRPS** kinematic chain (where the **RR** stands for the degrees of freedom that belongs to an universal joint, **P** is a prismatic degree of freedom that belongs to the linear power actuator, and **S** is the spherical joint that links the linear actuator with the final effector).

2.1 Inverse kinematic solution of a RRPS platform.

The inverse kinematic solution, that is calculated from the position and orientation of the final effector, allow us to get the necessary command variables to fit with a programmed path planning. The inverse geometric model of a RRPS platform consist of establishing the values of the joint variables of the kinematic chain from the configuration of the final effector. The raising of the solution can be easily obtained from the next vector description on generalized coordinates.

$$r_{ABi} = r + A_c s_i' - s_0 \qquad (1)$$

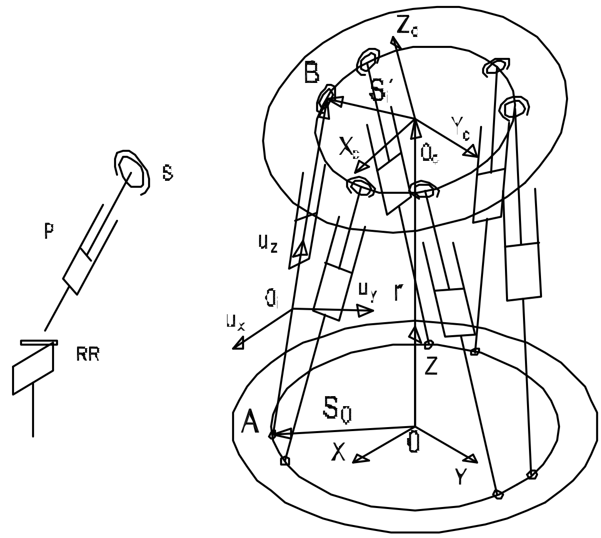

Figura-1 General structure of a 6 DOF parallel manipulator

Where $\boldsymbol{0}$ is the origin of the reference system of the base, $\boldsymbol{0_c}$ is the origin of the reference system of the center of the final effector. The generalized coordinates vector of the center of the final effector is: $\boldsymbol{q_c = [r, y_c, a_c, f_c]^T}$, $\boldsymbol{A_c}$ is the 313 Euler rotation matrix, $\boldsymbol{s'_i}$ and $\boldsymbol{s}_0$, are vectors relatives to the system $\boldsymbol{0_c}$ y $\boldsymbol{0}$ respectively. The $\boldsymbol{r_{ABi}}$ vectors are the joint variables that are calculated from the inverse solution, whose magnitude gives the configuration of the linear power actuators.

Based on the $\boldsymbol{r_{ABi}}$ vector norm, it is possible to determine the angles $\boldsymbol{y_i, a_i, f_i}$ of the generalised coordinates vector $\boldsymbol{q_i = [\, r_{ABi}, y_i, a_i, f_i \,]^T}$ For this purpose, for example, a reference system 0, with the u_Z axis aligned along the unitary vector of the $\boldsymbol{r_{ABi}}$ is fixed, as it is illustrated on Figure-1, so that:

$$\boldsymbol{u_Z} = \frac{\boldsymbol{r_{ABi}}}{\|\boldsymbol{r_{ABi}}\|}, \ \boldsymbol{u_X} = \frac{\boldsymbol{u_Z} ´ \boldsymbol{S}_0}{\|\boldsymbol{u_Z} ´ \boldsymbol{S}_0\|}, \text{ and } \ \boldsymbol{u_y} = \frac{\boldsymbol{u_Z} ´ \ \boldsymbol{u_X}}{\|\boldsymbol{u_Z} ´ \ \boldsymbol{u_X}\|}$$

From these unitary vectors, the matrix of director cosines can be obtained $\boldsymbol{A_i} = [\ \boldsymbol{u_X}, \boldsymbol{u_y}, \boldsymbol{u_Z}]$ and, from this, determine the angles $\boldsymbol{y_i, a_i, f_i}$, or the Euler parameters: $\boldsymbol{P} = \left[\boldsymbol{e}_0^i, \boldsymbol{e}_1^i, \boldsymbol{e}_2^i, \boldsymbol{e}_3^i\right]$ for the matrix $\boldsymbol{A_i} = \left(2\boldsymbol{e}_0^2 - 1\right)\mathrm{I} + 2\left(\boldsymbol{e}\,\boldsymbol{e}^T + \boldsymbol{e}_0\tilde{\boldsymbol{e}}\right)$

2.2 Numeric model for the direct kinematic solution.

The direct kinematics of a **RRPS** platform stablish the relations between the command variables of the linear actuators and the resultant position of the final effector.

There are, in specified literature, several methods for the geometric calculation of direct kinematic of 6 DOF parallel platforms, some of them allow us to get the possible solutions through the use of polynomials that result of the geometric modelling of the kinematic chains of the platform, for example in (8), the 16 possible solutions for a 6 DOF platform are calculated, (9) and (10) prove that the Stewart platform have 12 possible solutions. (11) suggest a systematic method to obtain the minimal polynomial equations for certain cases of parallel platforms, like for example a 3 DOF, with this method they obtain a solution of polynomials of 8 degrees, although for a general 6 DOF robot, the Nair's method arrives to polynomials of 144 degrees. For a general case of a 6 DOF platform, (12) prove that the maximum number of solutions is 40. On other hand, (13) suggest an approximation that reduces the problem to three equations plus one more equation of constraints that must be satisfied by the triplet of solutions and must be resolved by numerical methods. (14) offer a method for the polynomial formulation of order 40 for 6 DOF platforms, using rotation matrices based on quaternions, so that obtaining the geometric solutions of a 6 DOF platforms based on geometrical methods, implies a great number of calculations, that are incompatible with a real-time use.

In this section a numerical method based on the initial estimation of the generalized coordinates vector q_i will be exposed. In general, a 6 DOF RRPS parallel platform is formed by 12 links that constitute the linear actuators. Each couple of the previous links, are linked between them by a prismatic joint, and each one of the extremes are connected to the base and to the final effector through a spherical joint and an universal joint respectively. Then the generalized coordinates vector will be represented as: $\boldsymbol{q} = [\boldsymbol{q}_1, \boldsymbol{q}_2, \boldsymbol{q}_3, \; .... \; \boldsymbol{q}_{13}]^T{}_{91x1}$. Where $\boldsymbol{q}_1$ is the generalized coordinates system of the final effector and $\boldsymbol{q}_1, \boldsymbol{q}_2, \boldsymbol{q}_3, \; .... \; \boldsymbol{q}_{13}$ Correspond to the unit of generalized coordinates assigned to the couple of links that form the linear actuators. In general, each link is defined by a generalized coordinates system where: $\boldsymbol{q}_i = [\boldsymbol{r}_{ABi}, \boldsymbol{P}_i]^{\mathrm{T}}$ with $\boldsymbol{r}_{ABi} = [\boldsymbol{x}_i, \boldsymbol{y}_i, \boldsymbol{z}_i]$ and the Euler parameters: $\boldsymbol{P} = [\boldsymbol{e}_0^i, \boldsymbol{e}_1^i, \boldsymbol{e}_2^i, \boldsymbol{e}_3^i]$

The description of the kinematic chain of a RRPS, is based on the constraints vector:

$$f(q,t) = \begin{bmatrix} f^k(q) \\ f^D(q,t) \\ f^P(q) \end{bmatrix}_{91x1} = 0; \qquad (2)$$

Where $f^k(q)_{72x1}$ is the vector of the 72 holonomic constraints imposed by the prismatic, spherical and universal joints. $f^D(q,t)_{6x1}$ is a vector of 6 constraints imposed by the actuators, that in this case they are function of the command joint variables for which direct kinematics will be calculated. $f^P(q)_{13x1}$ is a vector of 13 constraints for the normalization of the Euler parameters.

2.2.1 Spherical Constraint

Spherical constraint restricts 3 degrees of freedom. They can be described as it is shown in Figure-2, and in the following equation:

$$f^{(s,3)}(p_i, p_j)_{3x1} = \boldsymbol{r}_j + \boldsymbol{A}_j \boldsymbol{s}_j'^{p} - \boldsymbol{r}_i - \boldsymbol{A}_i \boldsymbol{s}_i'^{p} = 0 \qquad (3)$$

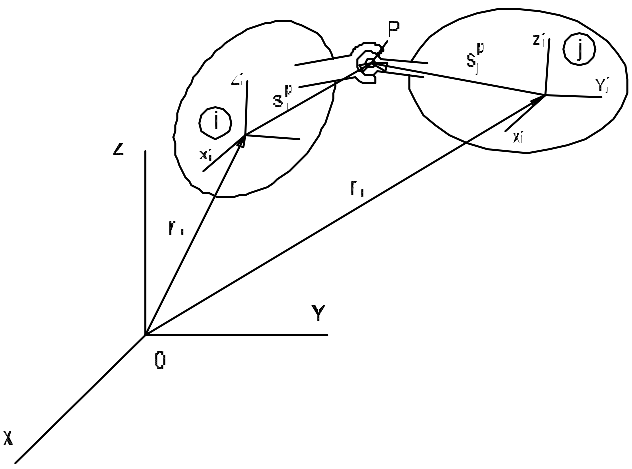

Figure-2. Spherical constraint

This type of constraint is defined describing a common point $\boldsymbol{p}$ of the spherical joint from the coordinates system x'_i, y'_i, z'_i and x'_j, y'_j, z'_j of the bodies i, j respectively.

2.2.2 Universal constraint

The universal constraint is shown in Figure-3. This type of constraint restricts 4 degrees of freedom, so that their description is based on the combination of a spherical constraint and the dot product of the unitary orthogonaly vectors $\boldsymbol{h}_i$ and $\boldsymbol{h}_j$, (with $\boldsymbol{h}_i = \boldsymbol{A}_i \boldsymbol{h}'_i$). This constrain gives the following equation:

$$f^{s}(\boldsymbol{p}_i, \boldsymbol{p}_j)_{3x1} = 0 \qquad (4)$$

$$f^{(d,1)}(\boldsymbol{h}_i, \boldsymbol{h}_j)_{1x1} = \boldsymbol{h}_i^T \boldsymbol{h}_j = \boldsymbol{h}_i'^T \boldsymbol{A}_i^T \boldsymbol{A}_j \boldsymbol{h}'_j = 0 \qquad (5)$$

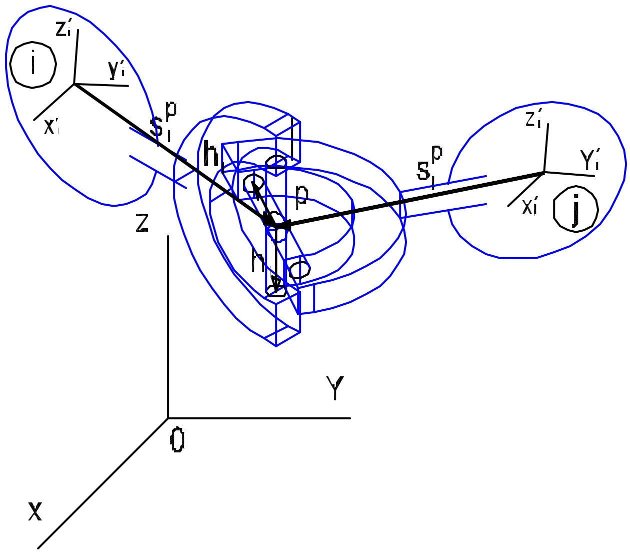

Figure-3. Universal constraints

2.2.3 Traslational constraint

The traslational restriction is used to describe the prismatic joints of the linear actuators. The description of this constraint is based on the vector product of $\boldsymbol{h}_i$, $\boldsymbol{h}_j$ and $\boldsymbol{d}_{ij}$, and the dot product of the unitary orthogonal vectors $\boldsymbol{f}_i$ and $\boldsymbol{f}_j$.

$$f^{(p,2)}(\boldsymbol{h}_i, \boldsymbol{h}_j)_{2x1} = 0 \quad (6)$$

$$f^{(p,2)}(\boldsymbol{h}_i, \boldsymbol{d}_{ij})_{2x1} = 0 \quad (7)$$

$$f^{(d,1)}(\boldsymbol{f}_i, \boldsymbol{f}_j)_{1x1} = \boldsymbol{f}_i'^T \boldsymbol{A}_i^T \boldsymbol{A}_j \boldsymbol{f}'_j = 0 \qquad (8)$$

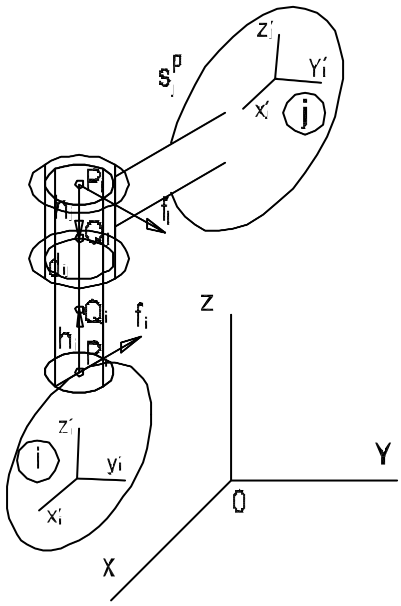

Figure-4. Traslational constraint

2.2.4 Constraints of the normalisation of the Euler parameters

The description of the multibody reference system in terms of Euler parameters force us to establish constraints for the normalization of these parameters, and they are written as:

$$f_i^P = p_i^T \, p_i - 1 = 0 \qquad (9)$$

The constraints of actuation $f^D(q,t)_{6x1} = 0$ are used to obtain the direct kinematic solution of a RRPS platform. According to Figure-5,

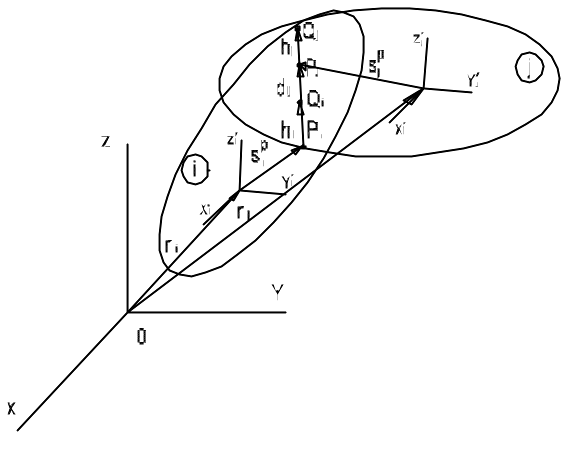

Figure-5. Relative traslational constraints of a linear actuator

Bodies i, j form the linear actuator with a traslational joint that is described through the points $\boldsymbol{P}_i$, , and $\boldsymbol{P}_j$. The unitary vectors $\boldsymbol{h}_i$ and $\boldsymbol{h}_j$ are built between the couples of points $\boldsymbol{P}$ and $\boldsymbol{Q}$.

The constraint of the traslational actuator can be written as the dot product of two co-linear vectors (if the vector $\boldsymbol{d}_{ij} \neq 0$) minus a $C_{ij}(t)$ function that represents the displacement of the linear actuator for which the direct solution is being calculated.

$$f^D = (\boldsymbol{h}_i, \boldsymbol{d}_{ij})_{1x1} = \boldsymbol{h}_i^T \boldsymbol{d}_{ij} - C_{ij}(t) \qquad (10)$$

The unitary vector h_i can be written as: $\boldsymbol{h}_i^T = \boldsymbol{h}_i^{'T} \boldsymbol{A}_i^T$ and $\boldsymbol{d}_{ij} = \boldsymbol{r}_j + \boldsymbol{A}_j \boldsymbol{s}'^P_j - \boldsymbol{r}_i - \boldsymbol{A}_i \boldsymbol{s}'^P_i$, where vectors with inverted comma are referred to the systems i and j fix together to each body, as it is shown in Figure-5, where $\boldsymbol{A}_i$ and $\boldsymbol{A}_j$ are the rotation matrices in terms of the director cosines of each system.

2.3 Numerical calculation of the kinematic solution

As it was mentioned before, to calculate the direct kinematic solution we start from an approximated generalized coordinates vector $\boldsymbol{q}_i$, and the displacement values $C_{ij}(t)$ (that for the case of the direct kinematic solution, depends only on the command variable). For these effects, it is commonly used the Newton-Raphson method.

$$f_q \Delta \boldsymbol{q}^{(j)} = - f(\boldsymbol{q}^{(j)}, t) \qquad (11)$$

$$\boldsymbol{q}^{j+1} = \boldsymbol{q}^{(j)} + \Delta \boldsymbol{q}^{(j)} \qquad (12)$$

Where f_q is the Jacobian of the vector of constraints described in (2) and $\boldsymbol{q}^{(j+1)}$ is the direct kinematic solution when $\Delta \boldsymbol{q}^{(j)} \approx 0$.

3. MECHANICAL ARCHITECTURES FOR PARALLEL CLIMBING ROBOTS

The studied mechanical architectures that are presented in this paper, are related to parallel robots that can move through metallic structures, face of buildings, inside tubes and climbing for the outer side of posts or cables.

3.1 Climbing robots for displacing over structures

Next figures show different kinematics configurations for parallel climbing robots that can manoeuvre over metallic structures of bridges or buildings. In all the cases, mechanical architectures are based on RRPS platforms, made of a couple of rings linked between them by linear power actuators.

Figures-6 and 7 show different kinematic configurations that prove the ability of parallel platforms to climb over structures, adjusting completely to the complex geometry of the structures.

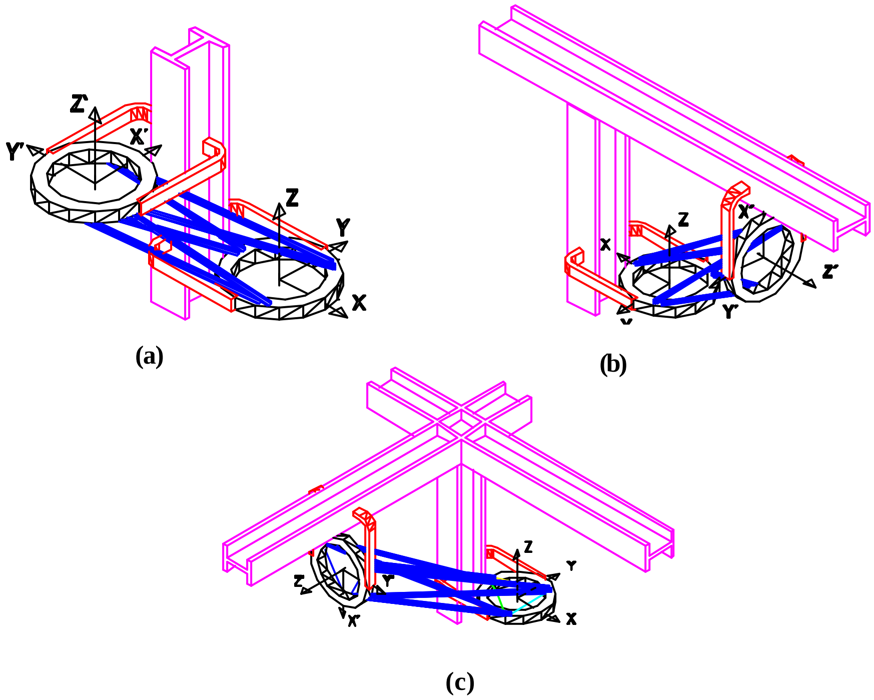

Figure-6. Three images that show the maneuver of a parallel robot over a structure. At (c) configuration, an interference between the intermediate linear power actuators appear.

Figure-6 (b), show the suggested solution for the parallel platforms that should manoeuvre over bridges or building structures. Take note that an additional degree of freedom on each ring has been additioned, with the purpose of solving the interference problems between the linear actuators that can appear in some configurations. From the point of view of control, teleoperation of this robots with base on a parallel master robot will allow us to solve directly complex problems that the direct kinematic solution create, the singularities and the reachable spaces inside the working universe of the robot.

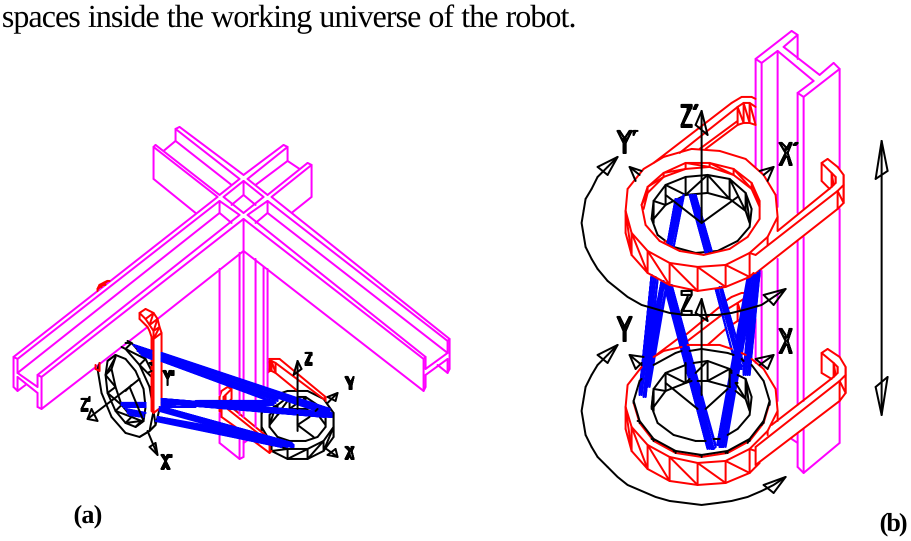

Figure-7 (a) shows a configuration that solves the interference between the linear actuators, letting the superior ring to achieve an orientation 45° out of phase respect the configuration (c) of the Figure-6.

3.2 Climbing robots for building fronts and surfaces

For this applications, it can be deduced that a 6 DOF parallel architecture, as one's shown in Figure-6 (a) is perfectly possible. In general, applications in these cases are numerous, and go from the cleaning of fronts, welding inspection of boats. Remembering that this type of robots has a great load capacity, so it is not difficult to foresee that they can carry weight welding systems or other types of mechanization tools remotely operated. At each specific case, subjection legs and handler arms for the tool, must be adapted to the basic platform, as shown in the next section.

3.3 Climbing robots for posts and cables.

The maintenance of posts, cables and large cylindrical structures with regular or irregular sections (like palm trees) in general require robots capable of climbing and orientating itself on the workspace, with the goal of being capable of adapting to curvature variations that this type of structures present.

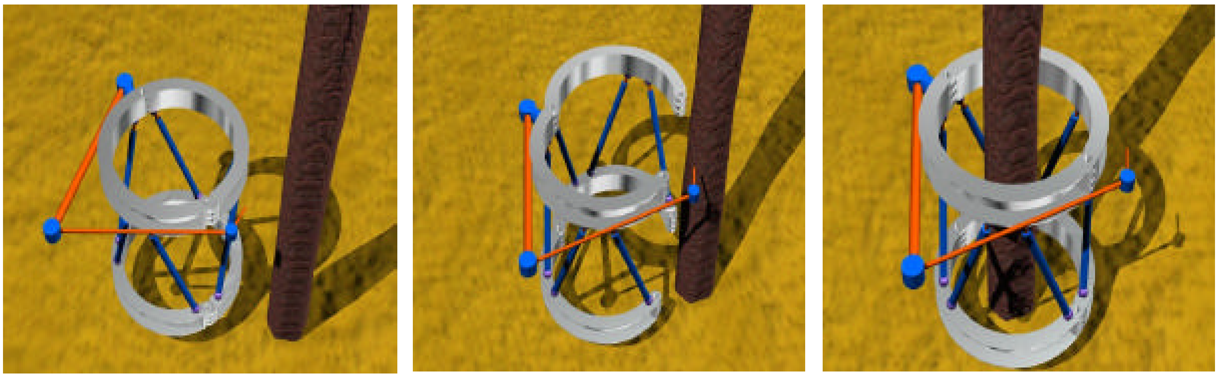

Figure-3.3 Architecture of a parallel climbing robot with a manipulator arm for large structures

The authoring group of this paper is developing this type of robot for the maintenance of posts, electrical cables and palm trees. The new advances in the investigation of the project TREPA, have allowed us to insert a manipulator arm for handling tools. At the extreme of the manipulator arm is predicted to insert a vision system for remote operation of the robot, and it is also being developed a master robot for teleoperation of the manipulator arm with bilateral force control.

4. DYNAMIC SIMULATIONS OF TYPICAL CONFIGURATIONS FOR PARALLEL CLIMBING ROBOTS

Several simulations have been developed for calculating the inverse dynamics and the capacity of the linear actuators. Models and simulations have been developed using ADAMS 9.1 software. The model of the robot used in the simulations is according with the morphology shown in Figure-7(b), where the holding grippers can be oriented according to the configuration of the structure while the robot is navigating. Physical characteristics of the simulated robot are shown in next table, these are initial values, so the weight of some components of the robot is not optimized.

The load capacity is supposed to be 25 kg. for a maximum displacement of 800 mm and a velocity of 0.4 m/sec.

Table 1 Technical specifications for the model of the parallel climbing robot

No.	Item	Description
1	Degrees of freedom	6
2	Material	Duraluminium 6063 T5
3	Actuators	Double effect pneumatic cylinders with 63 mm. of diameter
4	Pneumatic control valves	5/3 directional valves and flow control servovalves
5	Rings (final effectors)	Tip-up rings with hinge and automatic close, and pneumatic cylinders for centring, with force regulation
6	Diameter of rings	400 mm
6	Displacement capacity per cycle	800 mm.
8	Climbing velocity	0,4 M/Seg.
9	Payload capacity	25 Kg.
10	Maximum power required	1800 w
11	Payload/ Weight, ratio	0.5
12	Approximate total weight of the climbing robot (whithout payload)	50 Kg.

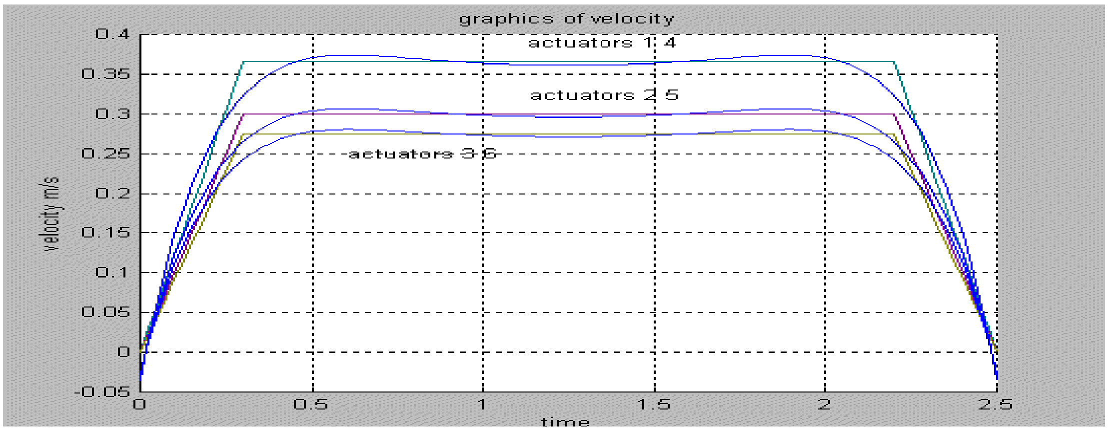

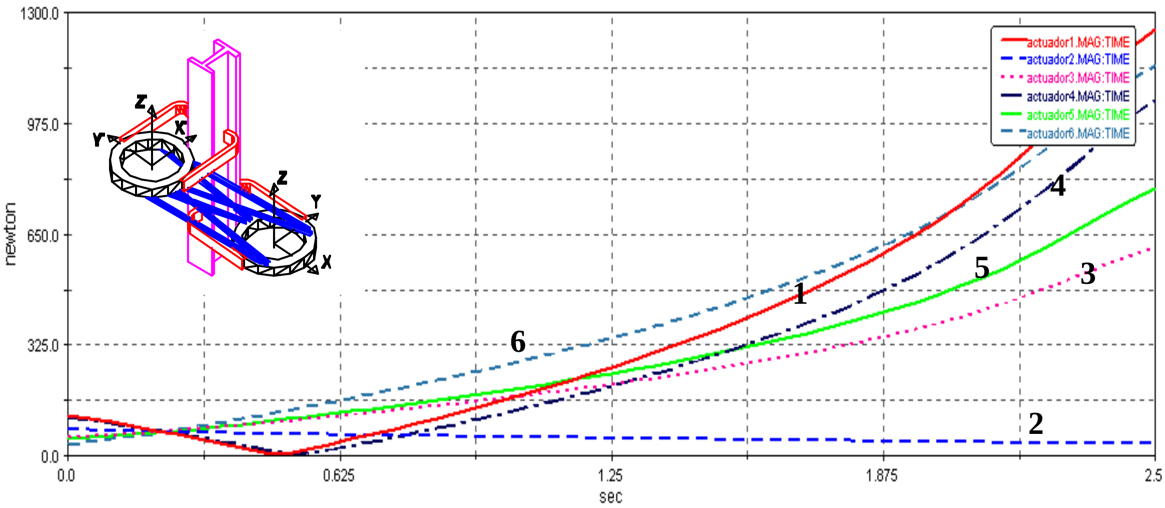

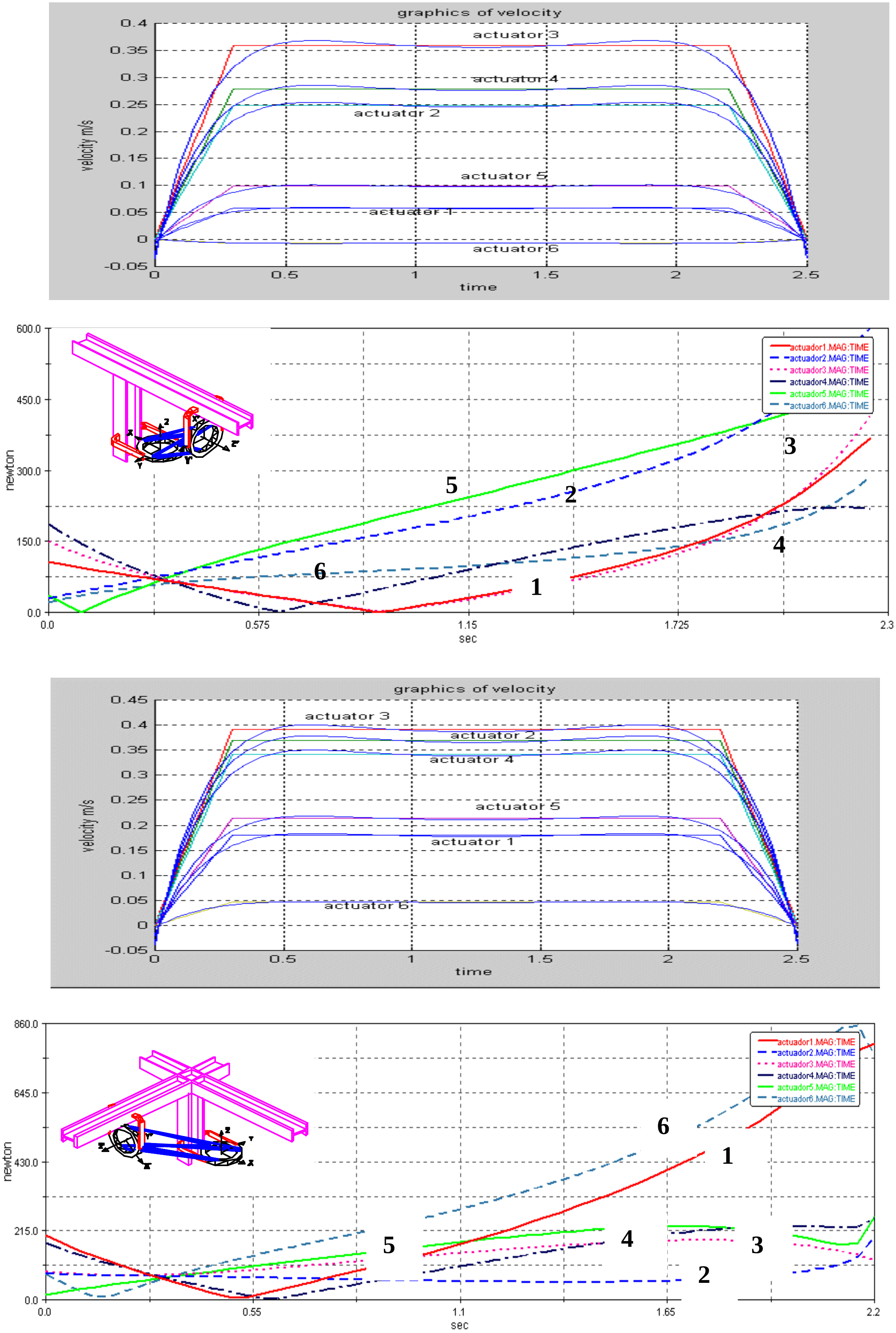

Figure-8. Profile of velocities (Path Planing) and forces required in the linear actuators for the path planning calculated for this simulation.

The path planning for the simulations were calculated with Matlab, following the models explained in the section 2 of this paper. According to the results of the simulations, the theoretic maximum power required is presented for the first case of the Figure-8, and if about 1800 w. The useful load charge is 25 kg., and is concentrated on the center of the moving ring. Take notice that in the former displacements, the dynamic effects of the load are critical, but in a parallel structure capable of changing the simulated configurations in one step, these effects can be assumed without difficulty.

5. CONCLUSIONS

On this paper, we have presented an advance in the investigations that nowadays have been taken place by the group of "Industrial Technologies" of "Miguel Hernández" University, for the development of parallel climbing robots dedicated to the maintenance of large structures like posts or cables. Applications of these robots to the maintenance of bridges or building structures have been also studied. For the study of the kinematics and dynamics of this type of platforms, computational object oriented tools in C++ have been developed in (20), using the multibody dynamics methods. With this develops we solve numerically the complex problems of the direct kinematic solutions, we also complete the necessary virtual dynamics scene for the remote teleoperation of this machines, and validate control strategies too. At the final of this paper several climbing robots architectures for bridges structures or large cylindrical structures have been proposed. Nowadays the fabrication of a prototype including a teleoperation system is being developed.

REFERENCES

(1) Cooke, D. S., Collie, A. A., Puttkamer, E. V., and Preumont, A. (1994). The design and performance of a pneumatic robot for walking/climbing vehicle. In *Hungarian-British Mechatrinics Conference*. Hungarian-British Mechatronics Conference.

(2) de Santos, P. G., M.A.Armada, and Jimenez, M. (1997). An industrial walking machine for naval construction. In *International Conference on Robotics and Automation*.

(3) A.Preumont and Alexandre, P. (1994). Some trends in walking robots in europe. In *Int. Conf. on Motion and Vibration Control MOVIC*, Yokohama,Japan.

(4) Bahr, B. and Yin, Y. (1994). Wall climbing robots for aircraft, ships, nuclear power planes, skyscrapers, etc. In *Robotics and Manufacturing*, volume 5, pages 377-382. ASME Press Series.

(5) Balaguer, C., Pastor, J., Giménez, A., Padrón, V., and Abderrahim, M. (1998). Roma: Multifunctional autonomous self-supported climbing robot for inspection applications. In *In proceedings of International Autonomous Vehicles,IAV'98*, Madrid, Spain.

(6) Billingsley, J., Collie, A., and Rook, M. (1993). An improved wall-climbing robot with minimal actuation. In *1st IFAC International Workshop on Intelligent Autonomous Vehicles*, pages 14-19. International Federation of Automatic Control.

(7) Merlet, J. P, Les Robots Parallèles, Ed. Hermes, 1997.

(8) Merlet, J. P. Direct kinematics and assembly modes of parallel manipulators. International Journal of Robotics Research, 11(2), 150-162, April 1992.

(9) Lazard, D., Merlet, J. P., Stewart platform has 12 configurations. In IEEE Int. Conf. On Robotics and Automation, pages 2160-2165, San Diego, May 8-13, 1994.

(10) Danescu G. et Dahan M., · Janvier 1994. Prolégomènes nº 6 (INRIA)
(11) Nair P. On the foward kinematics of parallel manipulators. The Int. J. Of Robotics Researc, 13(2):171-188, April 1994
(12) Lazard, D. Stewart platform and Gröbner basis. In ARK, pages 136-142, Ferrae, 7-9 September 1992.
(13) Dasgupta B., Mruthyunjaya, T. S., A canonical formulation of the direct position kinematics for a general 6-6 Stewart platform. Mechanism and Machine Theory, 29(6):819-827, Août 1994.
(14) Husty, M. L. An algorithm for solving the direct kinematic of Stewart-Gough type platforms, Rapport de Recherche TR-CIM-94-7, Universite McGill, Montreal, June 1994
(15) Nikravesh, P. E. Computer-Aided Analysis of Mechanical Systems, Prentice Hall, 1988
(16) Haug, E. J. Computer Aided Kinematics and Dynamics Of Mechanical Systems, Allyn and Bacon, 1989
(17) Wehage, R. A., Haug, E. J. Generalized Coordinate Partitioning for Dimension Reduction in Analysis of Constrained Dynamic System, Journal of Mechanical Design, Vol. 104, No. 1 pp 247-255, 1982
(18) Baumgarte, J. Stabilization of Constrains and Integrals of Motion, Computer Methods in Applied Mechanics and Engineering, Vol. 1 pp. 1-16, 1972
(19) Park T., An Hybrid Constraint Stabilization-Generalized Coordinate Partitioning Method for Machine Dynamics, Journal of Mechanisms, Transmission, and Automation in Design, Vol. 108 , No. 2, 1986, pp 211-216.
(20) Saltarén. R. P., Tools for modeling and parametric design of robots based on multibody dynamics, PhD Thesis, Polytechnic University of Madrid, 1996.